SUPPLEMENTAL INFORMATION

Inventory of Supplemental Information

Supplemental Figures

Figure S1 (Related to **Figure 1**). The interaction network of HSC20 includes SDHB, LYRM7, SUCLG2, NQO2, HELZ, EPRS.

Figure S2 (Related to **Figure 2**). The HSC20-HSPA9-ISCU complex targets SDHB and controls assembly of Complex II.

Figure S3 (Related to **Figure 4**). Prolonged knockdowns of HSC20 or HSPA9 affect stability of respiratory complex I-III subunits and alter iron metabolism (Panels A-E). Expression of a dominant negative mutant of HSC20, defective in HSPA9 activation, impairs SDH assembly (Panels F-L).

Figure S4 (Related to **Figure 5**). Helices 1 and 2 (residues 158- 177 and 175- 206, respectively) in the C-terminal domain of HSC20 mediate the interaction with SDHB.

Figure S5 (Related to **Figure 6**). Two L(I)YR motifs in SDHB are bound by HSC20 and are critical for SDH assembly.

Figure S6 (Related to **Figure 7**). HSC20 interacts with GLRX5 *in vivo*.

Supplemental Tables

Table S1 (Related to **Figure 1**). List of proteins that were found to interact with HSC20.

Table S2 (Related to **Figure 5**). List of HSC20 clones assayed by Y2H for the interaction with SDHB.

Table S3 (Related to **Figures 6 and 7**). List of SDHB clones assayed by Y2H for the interaction with HSC20.

Table S4 (Related to the **Experimental Procedures**). List of plasmids used in this study for transfection of human cells.

Table S5 (Related to **Figure 6**). Multiple Sequence Alignments: five multiple sequence alignments were performed to show conservation of the LYR motif in subunits of respiratory Complex I and in SDHB in humans, yeast, plants and bacteria.

Supplemental Experimental Procedures

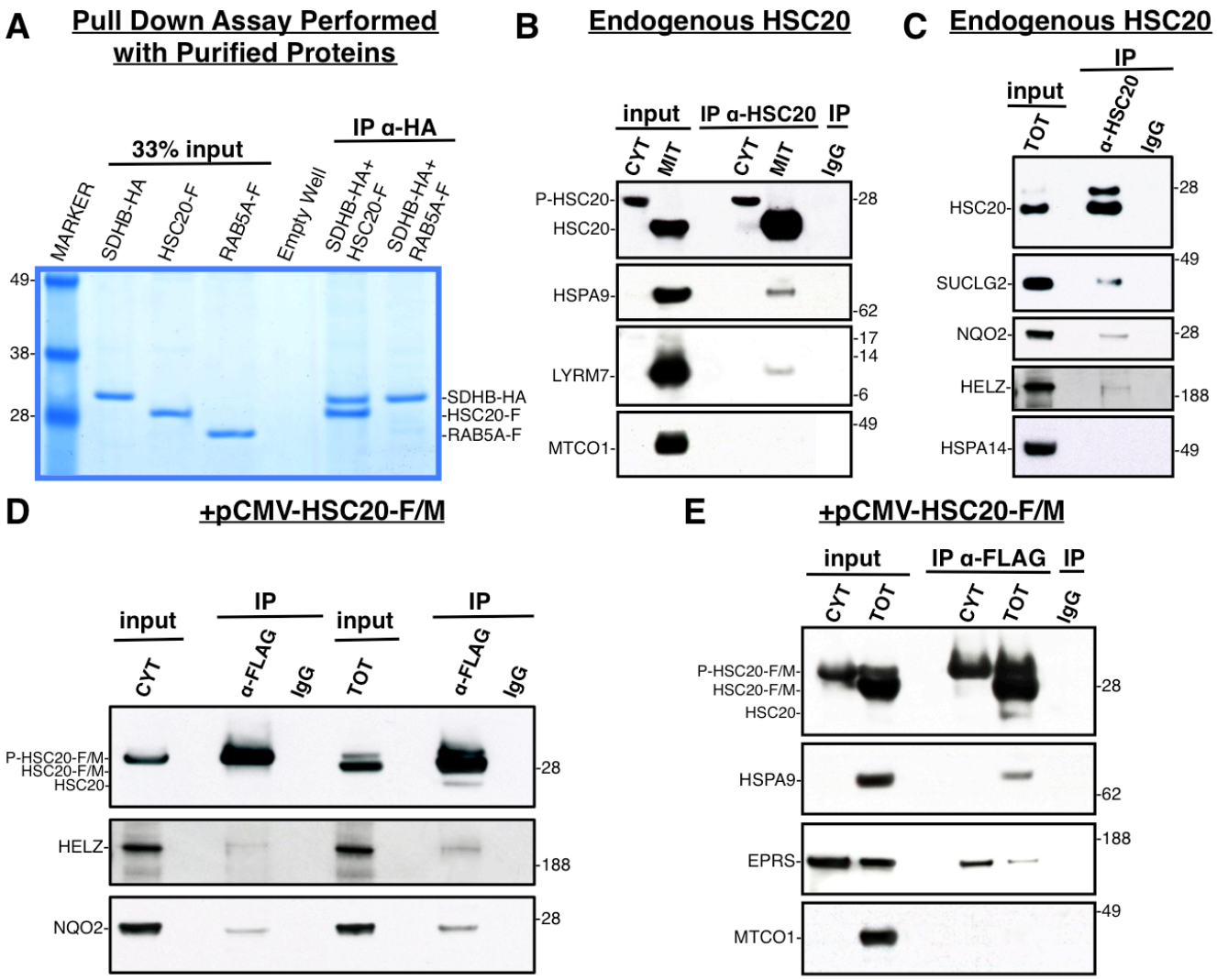

Figure S1, Related to Figure 1. The Interaction Network of HSC20 Includes SDHB, LYRM7, SUCLG2, NQO2, HELZ, EPRS. (A) Pull down assay with purified proteins. 30 µg of purified SDHB-HA were combined with 30 µg of either HSC20-FLAG (HSC20-F) or RAB5A-FLAG (RAB5A-F), as indicated, in buffer I2 (25 mM TrisHCl; 300 mM NaCl; 1 mM EDTA; 1% NP-40; 1% DTT; 1 mM PMSF; 5% glycerol). RAB5A-F was used as a negative control. IPs were performed with anti-HA antibodies to immunoprecipitate SDHB-HA. The presence of co-IPed HSC20-F or RAB5A-F was analyzed by SDS-PAGE and Coomassie staining. Aliquots corresponding to 33% of the inputs were run on the gel for comparison. Purified SDHB-HA bound to purified HSC20-F, indicating direct interaction. (B) Eluates after IP of endogenous HSC20 on cytosolic (CYT) or mitochondrial (MIT)

fractions from HEK293 were probed with antibodies to HSC20 (P-HSC20, HSC20 precursor before cleavage of the mitochondrial targeting sequence, MTS), HSPA9, LYRM7, and MTCO1 (COX1, Complex IV subunit). (C) Eluates after IP of endogenous HSC20 on total lysates from HEK293 were probed with antibodies to SUCLG2, NQO2, HELZ and HSPA14 to search for possible interactions. (D) IP of HSC20-F/M on cytosolic (CYT) or total (TOT) extracts from HEK293 transfected with pCMV-HSC20-F/M and evaluation of interactions with endogenous HELZ and NQO2. (E) IP of HSC20-F/M on cytosolic (CYT) or total fractions (TOT) from HEK293 transfected with pCMV-HSC20-F/M and evaluation of interactions with endogenous HSPA9, EPRS, MTCO1. Inputs were 30% of total used for the IPs.

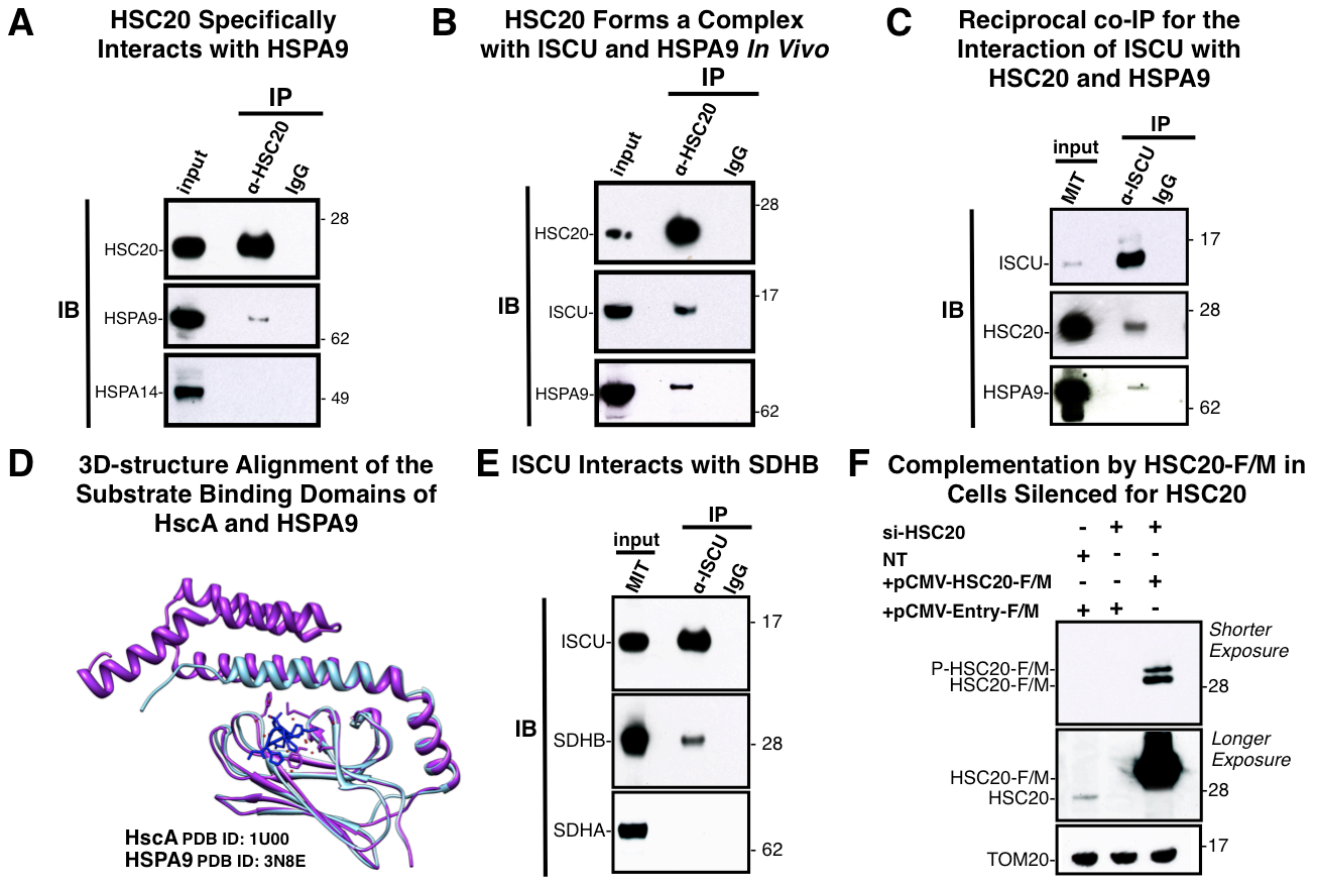

Figure S2, Related to Figure 2. The HSC20-HSPA9-ISCU Complex Targets SDHB and Controls Assembly of Complex II. (A) HSC20 specifically interacts with HSPA9. IP of HSC20, followed by IBs to HSPA9 or HSPA14 (a negative control). (B) HSC20 forms a complex with ISCU and HSPA9 *in vivo*. IP of HSC20, followed by IBs to ISCU and HSPA9. (C) Reciprocal co-IP confirming the interaction of ISCU with HSC20 and HSPA9. IP of ISCU, followed by IBs to HSC20 and HSPA9. In A-C inputs were 10- 30% of total used in the IPs. (D) 3D-structure alignment of the substrate binding domains of HscA (in purple, PDB ID: 1U00) and HSPA9 (in cyan, PDB ID: 3N8E). (E) ISCU interacts with SDHB. IP of ISCU, followed by IBs to SDHB or to SDHA. Input was 30% of total used in the IP. (F) Complementation assay on cells silenced for HSC20 and re-transfected with pCMV-HSC20-F/M. 24 h after knockdown of HSC20, HEK293 cells were transfected with pCMV-HSC20-F/M. Lysates were prepared 48 h after the initial transfection with si-RNAs and the membrane was probed with antibodies to HSC20 or to TOM20 (TOM20) as a loading control.

A LEVELS OF SUBUNITS OF RESPIRATORY CHAIN COMPLEXES UPON KNOCKDOWN OF HSC20 OR HSPA9

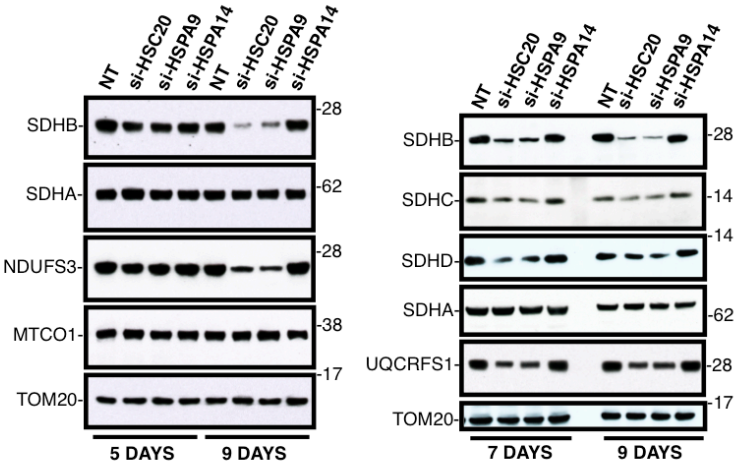

B BAND SHIFT UPON KNOCKDOWN OF HSC20 OR HSPA9

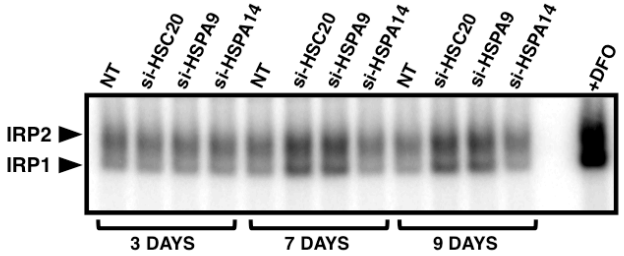

C ACONITASE ACTIVITIES UPON KNOCKDOWN OF HSC20 OR HSPA9

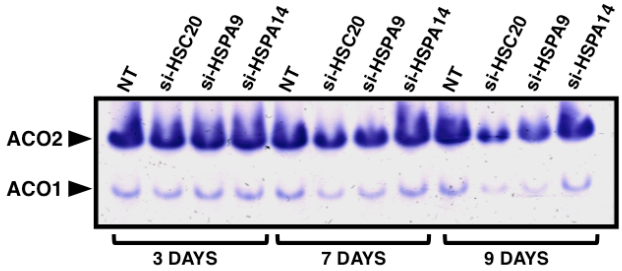

D IRP2 AND TFR1 LEVELS UPON KNOCKDOWN OF HSC20 OR HSPA9

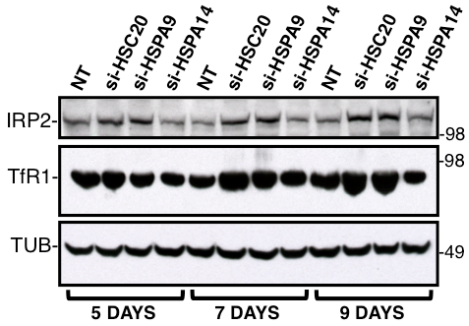

E EFFICIENCIES OF KNOCKDOWN OF HSC20, HSPA9 AND HSPA14

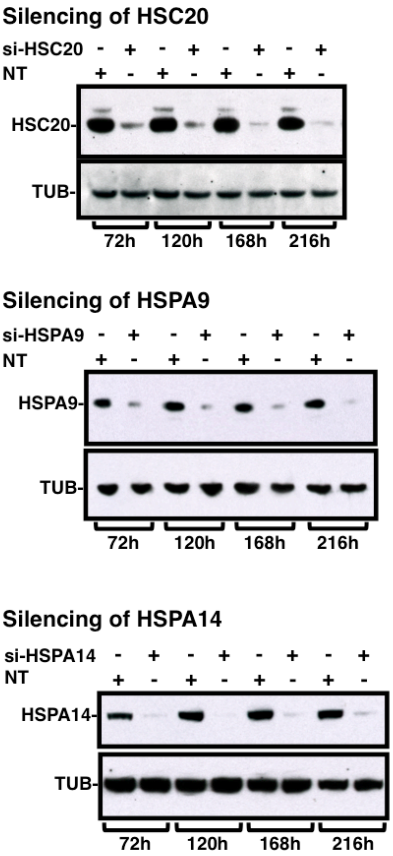

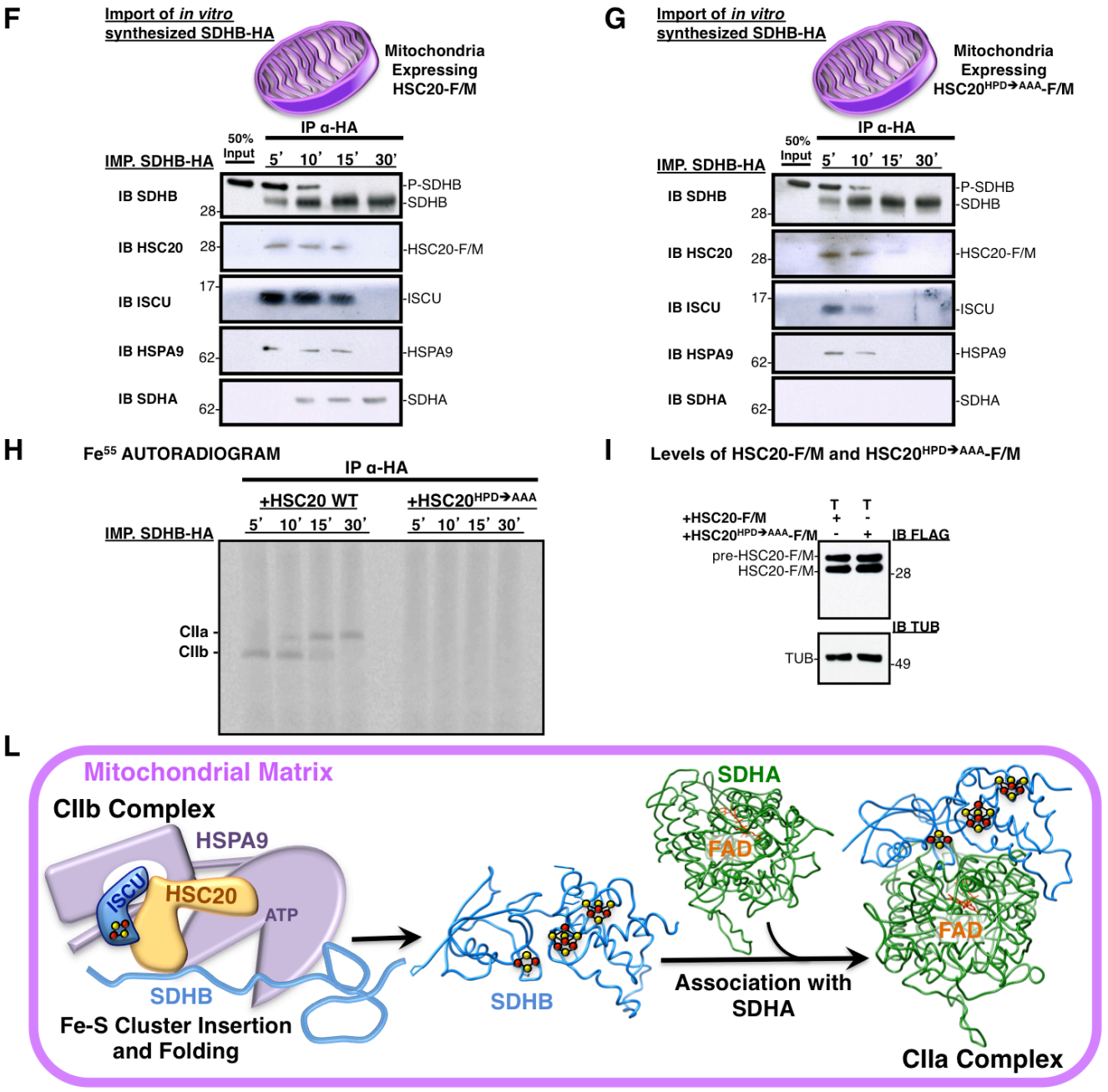

Figure S3, Related to Figure 4. Prolonged Knockdowns of HSC20 or HSPA9 Affect Stability of Respiratory Complex I-III Subunits and Alter Iron Metabolism (Panels A-E). Expression of a Dominant Negative Mutant of HSC20, Defective in HSPA9 Activation, Impairs SDH Assembly (Panels F-L).

(A) Levels of subunits of the respiratory chain complexes upon silencing of HSC20, HSPA9 or HSPA14 for 5, 7, or 9 days. All four Complex II subunits were detected with antibodies to SDHA,

SDHB, SDHC and SDHD. NDUFS3 levels were checked for Complex I. Cytochrome c oxidase subunits I (MTCO1) was detected for Complex IV, and levels of the Rieske Fe-S protein, UQCRFS1, were detected for Complex III. (B) IRE binding assay of IRP1 and IRP2 and (C) in-gel aconitase activities in cells silenced for HSC20 (si-HSC20), HSPA9 (si-HSPA9) or HSPA14 (si-HSPA14) for 3, 7 or 9 days. (D) IRP2 and TfR1 levels in cells silenced for HSC20, HSPA9 and HSPA14 for 5, 7 or 9 days. IB to tubulin (TUB) was performed to check for equal loading. (E) Efficiencies of HSC20, HSPA9, HSPA14 knockdowns. (F) Mitochondria isolated from HEK293 transfected with pCMV-HSC20-F/M or with pCMV-HSC20$^{HPD\text{-}AAA}$–F/M (panel G) were incubated with equal amounts of *in vitro* synthesized SDHB-HA for the indicated time points (5', 10', 15', 30'). Mitochondrial matrix extracts were prepared, and the IP was performed with anti-HA antibody to immunoprecipitate SDHB-HA (P-SDHB, SDHB-HA precursor before cleavage of the MTS). Eluates were probed with antibodies to SDHB, HSC20, ISCU, HSPA9 and SDHA (50% of *in vitro* synthesized SDHB-HA (input) was loaded onto the gel for comparison). (H) Fe^{55} labeling of SDHB-HA imported for the indicated time points into mitochondria isolated from cells transfected with pCMV-HSC20-F/M (+HSC20-F/M) or with pCMV-HSC20$^{HPD\text{-}AAA}$–F/M (+HSC20$^{HPD\text{-}AAA}$–F/M). The IP was performed with anti-HA antibody on the mitochondrial matrix fraction, followed by elution with 20 μg/ml of HA peptide in order to compete out SDHB-HA from beads without perturbing the native conformation of the protein and the retention of the clusters enclosed into mature SDHB. (I) Levels of expression of HSC20-F/M or HSC20$^{HPD\text{-}AAA}$–F/M on total lysates (T) from HEK293 transfected with pCMV-HSC20-F/M or pCMV-HSC20$^{HPD\text{-}AAA}$–F/M. (L) Schematic diagram of steps that lead to transition of SDHB from complex CIIb to CIIa upon successful insertion of Fe-S clusters by the chaperone-cochaperone transfer apparatus.

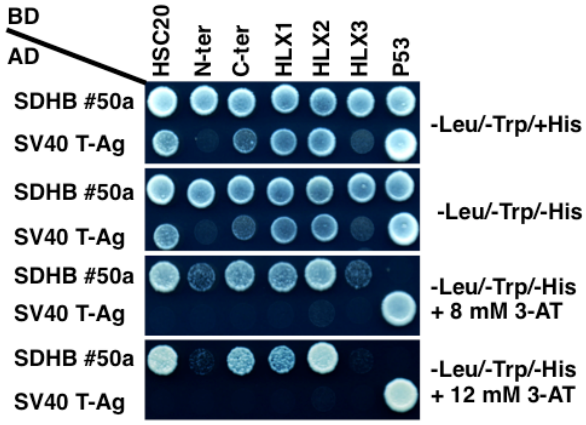

Figure S4, Related to Figure 5. Helices 1 and 2 (residues 158- 177 and 175- 206, Respectively) in the C-terminal Domain of HSC20 Mediate the Interaction with SDHB. Helices 1 (HLX1) and 2 (HLX2) in the C-terminus (C-ter) of HSC20 mediate the interaction with SDHB. Five truncated mutants of HSC20 were generated and used in the Y2H assay to test their interaction with SDHB clone #50a. (n = 5 biological samples). See Table S2.

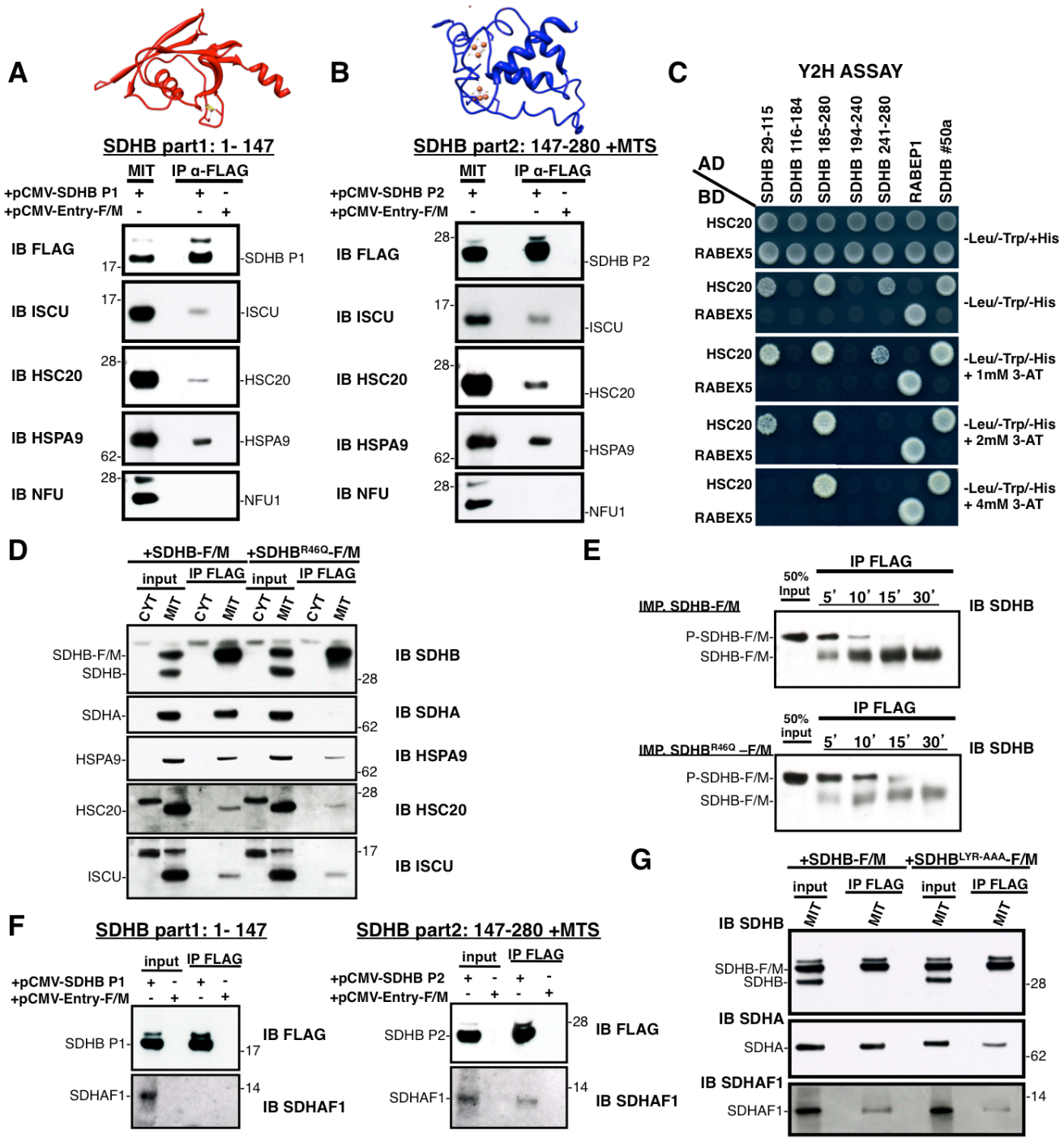

Figure S5, Related to Figure 6. Two L(I)YR Motifs in SDHB are Bound by HSC20 and are Critical for SDH Assembly. (A, B) Extracts from cells transfected with pCMV-SDHB P1 (residues 1-147 of SDHB F/M-C-terminally tagged) or with pCMV-SDHB P2 (residues 147- 280 of SDHB F/M-C-terminally tagged and engineered to have the MTS at the N-terminus), were subjected to IP with

anti-FLAG and the eluates were probed for the presence of HSC20, ISCU, HSPA9 or NFU1. Both domains of SDHB bound the HSC20-ISCU-HSPA9 complex. Inputs were 30% of total used in the IPs. (C) Y2H screen of five regions of SDHB covering residues 29- 115, 116- 184, 185- 280, 194- 240, 241- 280, as indicated, and expressed as fusions to GAL4-AD. HSC20 was used as a bait to screen the ability of binding of the five different clones of SDHB. (D) Effect of R46Q mutation of SDHB on binding to the chaperone-cochaperone transfer complex and to SDHA. IP of SDHB-F/M or $SDHB^{R46Q}$–F/M, followed by IBs to SDHA, HSPA9, HSC20, or ISCU. Inputs were 30% of total used in the IPs. (E) Effect of R46Q mutation of SDHB on the stability of the protein. *In vitro* synthesized SDHB-F/M or $SDHB^{R46Q}$–F/M were imported into isolated mitochondria for the indicated time points. Lysates were made and assayed by IB to SDHB, after IP with anti-FLAG. (P-SDHB-F/M, SDHB-F/M precursor before cleavage of the MTS). (F) SDHAF1 interacts with the C-terminus of SDHB. IP of SDHB part1 (1-147) or SDHB part2 (147-280) on mitochondrial extracts, followed by IBs to SDHAF1. (G) SDHAF1 interacts with SDHB through a non-LYR binding site. IP of SDHB-F/M or $SDHB^{LYR-AAA}$–F/M on mitochondrial extracts, followed by IBs to SDHA or to SDHAF1. In F and G inputs were 40% of total used in the IPs. See Table S3.

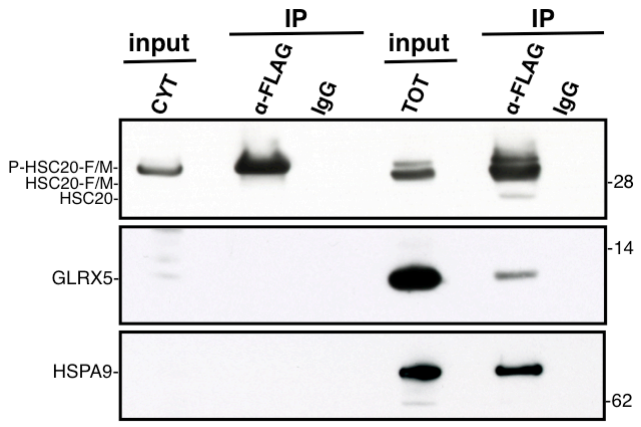

Figure S6, Related to Figure 7. HSC20 Interacts with GLRX5 *in vivo*. IP of HSC20-F/M on cytosolic (CYT) or total (TOT) extracts from HEK293 transfected with pCMV-HSC20-F/M and evaluation of interactions with endogenous GLRX5 and HSPA9. Inputs were 30% of total used in the IPs.

Table S1, Related to Figure 1. List of Proteins that were Found to Interact with HSC20. HSC20-BD-GAL4 was used as a bait to screen a human cDNA library from HeLa cells. 54 total candidates were identified as HSC20 interacting partners. Multiple putative interacting partners were validated by co-IP (**Co-IP**[a]: **+** = interaction validated by co-IP; **-** = no interaction; **ND** = Not Determined).

Table S2, Related to Figure 5. List of HSC20 Clones Assayed by Y2H for the Interaction with SDHB. Different HSC20 regions, as indicated, were cloned into pGBKT7 and used as baits to test their ability to interact with SDHB #50A (residues 104- 280).

HSC20 REGION (Cloned into pGBKT7)	Y2H Results with SDHB #50a into pGADT7
HSC20 29- 235	POSITIVE
N-ter 29- 159	NEGATIVE
C-ter 160- 235	POSITIVE
HLX1 158- 177	POSITIVE
HLX2 175- 206	POSITIVE
HLX3 206- 235	NEGATIVE
HLX1/2 158- 206	POSITIVE
HLX 2/3 175- 235	POSITIVE
HLX 1/3 158- 177/ 206- 235	NEGATIVE

Table S3, Related to Figures 6 and 7. List of SDHB Clones Assayed by Y2H for the Interaction with HSC20. Different SDHB regions, as indicated (i.e. SDHB 29- 115 encodes residues 29- 115 of human SDHB), were cloned into pGADT7 and screened for their ability to interact with HSC20 (used as a bait and cloned into pGBKT7). Point mutations were introduced, as indicated.

SDHB REGION / # Clone into pGADT7	Y2H Results with HSC20 into pGBKT7
SDHB 29- 115 / #1	POSITIVE
SDHB 116- 184 / #2	NEGATIVE
SDHB 185- 280 / #3	POSITIVE
SDHB 1- 90 / #4	POSITIVE
SDHB 194- 240 / #5	NEGATIVE
SDHB 241- 280 / #6	POSITIVE
SDHB 185- 240 / #7	NEGATIVE
SDHB 185- 209 / #8	NEGATIVE
SDHB 185- 221 / #9	NEGATIVE
SDHB 194- 221 / #10	NEGATIVE
SDHB 202- 221 / #11	NEGATIVE
SDHB 202- 280 / #12	POSITIVE
SDHB 202- 246 / # 13	POSITIVE
SDHB 255- 280 / #14	POSITIVE
SDHB 71- 102 / #15	NEGATIVE
SDHB 35- 52 / #16	POSITIVE
SDHB 243-263 / #17	NEGATIVE
SDHB 238- 258 / #18	POSITIVE
SDHB 255- 280 ($K_{267}K_{268}$ → $A_{267}A_{268}$) / #19	NEGATIVE
SDHB 255- 280 (Δ276-280) / #20	NEGATIVE
SDHB 255- 280 ($K_{276}K_{277}$ → $A_{276}A_{277}$) / #21	NEGATIVE
SDHB 35- 52 ($I_{44}Y_{45}R_{46}$ → $A_{44}A_{45}A_{46}$) / #22	NEGATIVE
SDHB 238- 258 ($L_{240}Y_{241}R_{242}$ → $A_{240}A_{241}A_{242}$) / #23	NEGATIVE

SDHB 255- 280 ($T_{272}Y_{273}K_{274}$➔$A_{272}A_{273}A_{274}$) /#24	**NEGATIVE**
SDHB 194- 240 ($A_{215}Y_{216}R_{217}$ ➔ $L_{215}Y_{216}R_{217}$) / #25	**NEGATIVE**
SDHB 238- 258 ($L_{240}Y_{241}R_{242}$ ➔ $A_{240}Y_{241}R_{242}$) / #26	**NEGATIVE**
SDHB 35- 52 ($I_{44}Y_{45}R_{46}$ ➔ $A_{44}Y_{45}R_{46}$) / # 27	**NEGATIVE**
SDHB 185- 240 ($S_{198}Y_{199}W_{200}$ ➔ $L_{198}Y_{199}R_{200}$) / #28	**NEGATIVE**
SDHB 35- 52 ($I_{44}Y_{45}R_{46}$ ➔ $I_{44}Y_{45}Q_{46}$) / # 29	**POSITIVE**
SDHB 35- 52 (F_{42} ➔ A_{42}) / #30	**POSITIVE**
SDHB 202- 246 (F_{238} ➔ A_{238}) / #31	**POSITIVE**
SDHB 238- 258 (F_{238} ➔ A_{238}) / #32	**POSITIVE**
SDHB 35- 52 ($I_{39}K_{40}K_{41}$ ➔ $A_{39}A_{40}A_{41}$) / # 33	**POSITIVE**

Table S4, Related to the Experimental Procedures. List of Plasmids Used in this Study for Transfection of Human Cells

Plasmids Used in this Study for Transfection of Human Cells	Description
pCMV-Entry-F/M	Plasmid for expression of C-terminally tagged MYC/ FLAG ORFs
pCMV-HSC20-F/M	MYC-FLAG-tagged ORF clone of Human HSC20
pCMV-SDHB-F/M	MYC-FLAG-tagged ORF clone of Human SDHB
pCMV-NFU1-F/M	MYC-FLAG-tagged ORF clone of Human NFU1
pCMV-HSC20-N-ter-F/ M	MYC/FLAG-tagged ORF clone of Region 1- 159 of Human HSC20
pCMV-HSC20-N-ter-F/ M (Construct 2)	MYC/FLAG-tagged ORF clone of Region 1- 146 of Human HSC20
pCMV-HSC20-C-ter-F/M	MYC/FLAG-tagged ORF clone of Region 160- 235 of Human HSC20
pCMV-HSC20-C-ter-F/M (Construct 2)	MYC/FLAG-tagged ORF clone of Region 147- 235 of Human HSC20
pCMV-HSC20^{Y220A}-F/M	MYC-FLAG-tagged ORF clone of Human HSC20, harboring the indicated point mutation
pCMV-HSC20^{F221A}-F/M	MYC-FLAG-tagged ORF clone of Human HSC20, harboring the indicated point mutation
pCMV-HSC20^{Y220A_F221A}-F/M	MYC-FLAG-tagged ORF clone of Human HSC20, harboring the indicated point mutations
pCMV-HSC20^{L162A_M166A}-F/M	MYC-FLAG-tagged ORF clone of Human HSC20, harboring the indicated point mutations
pCMV-HSC20^{L162A_M166A_Y220A}-F/M	MYC-FLAG-tagged ORF clone of Human HSC20, harboring the indicated point mutations
pCMV-HSC20^{L162A_M166A_F221A}-F/M	MYC-FLAG-tagged ORF clone of Human HSC20, harboring the indicated point mutations
pCMV-HSC20$^{HPD\rightarrow AAA}$-F/M	MYC-FLAG-tagged ORF clone of Human HSC20, harboring the indicated point mutations
pCMV-SDHB-F/M Part1	MYC-FLAG-tagged ORF clone of Human SDHB, Region 1- 147
pCMV-SDHB-F/M Part2	MYC-FLAG-tagged ORF clone of Human SDHB, Region 147-280
pCMV-SDHB^{R46Q}-F/M	MYC-FLAG-tagged ORF clone of Human SDHB, harboring the indicated point mutation
pCMV-SDHB$^{IYR-AAA}$-F/M	MYC-FLAG-tagged ORF clone of Human SDHB, harboring the indicated point mutations
pCMV-SDHB$^{LYR-AAA}$-F/M	MYC-FLAG-tagged ORF clone of Human SDHB, harboring the indicated point mutations

Table S5, Related to Figure 6. Multiple Sequence Alignments

Multiple sequence alignments were performed to show conservation of the LYR motif in subunits of Complex I (NADH dehydrogenase), and Complex II (succinate dehydrogenase) in humans, yeast, plants and bacteria.

For Complex I, the nomenclature and the number of subunits greatly differs between eukaryotes and prokaryotes.

In eukaryotes, we found that NDUFS8, a core component of the mitochondrial respiratory chain Complex I that is predicted to bind two [4Fe-4S] clusters, contains a highly conserved LYR motif. Thus far, two annotated members of the LYR family, NDUFA6 (LYRM6) and NDUFB9 (LYRM3), are known to be Complex I subunits.

In prokaryotes, Complex I genes and derived proteins are called *NuoA- N* (from NADH- ubiquinone oxidoreductase) or *Nqo1- 14* (from NADH- quinone oxidoreductase). We analyzed prokaryotic Complex I subunits and found that NuoM, NuoN, Nqo13 and Nqo14 contain highly conserved LYR motifs. Multiple sequence alignments are reported for these subunits.

SUPPLEMENTAL EXPERIMENTAL PROCEDURES

Complex I and Complex II Activities

In- gel Complex I and Complex II activities were performed as described (Diaz et al., 2009; Wittig et al., 2007). Briefly, for Complex I activity, after resolution of the respiratory chain complexes on BN-PAGE, the gel was incubated with 0.1 M TrisCl, pH 7.4, containing 1 mg/ml nitrobluetetrazolium chloride (NBT) and 0.14 mM NADH at room temperature for 30- 60 min. For Complex II, succinate dehydrogenase (SDH) activity (MES- mediated NBT reduction), the gel was incubated for 30 minutes with 84 mM succinate, 2 mg/ml NBT, 4.5 mM EDTA, 10 mM KCN, 1 mM sodium azide and 0.2 mM phenazine methosulphate (MES) in 50 mM PBS, pH 7.4. Detection of Complex II succinate CoQ-reductase activity (SQR) required addition of 10 μM ubiquinone, while no

MES was used. The spectrophotometric assay method for determining Complex II SDH activity (MES-mediated reduction of iodonitrotetrazolium chloride, INT) was performed as described (Munujos et al., 1993). Complex II SQR activity (CoQ- dependent reduction of INT) was determined as described (Lemarie et al., 2011). The spectrophotometric assay used for determining Complex I activity was based on an ELISA microplate kit from Mitosciences (ab109721).

Iron incorporation assay

The Fe^{55} incorporation assay into the mitochondrial respiratory chain complexes was done essentially as described (Stehling et al., 2009), with several modifications. Briefly, after two transfections (at 24 hours of interval) with si-RNAs to knockdown HSC20, HSPA9, or HSPA14, as indicated, cells were grown in the presence of 1 μM Fe^{55}-Tf for three days. Cell extracts were subjected to BN-PAGE, followed by autoradiography. On BN-PAGE, Complex I is detectable only as part of a supercomplex (S1), as already described (Stehling et al., 2009).

Pull Down Assay Performed with Purified Proteins

Human SDHB-HA (residues 29-280 + HA tag at the C-terminus), human HSC20-FLAG (residues 29-235 + FLAG tag at the C-terminus), and human RAB5A-FLAG (residues 1-215 + FLAG at the N-terminus, used as a negative control) were cloned into pEXP5-CT/TOPO vector for the expression in the cell-free *E. coli* system. Proteins were purified from the reaction mix by using anti-HA (for SDHB-HA) or anti-FLAG (for HSC20-FLAG or RAB5A-FLAG) antibodies covalently conjugated onto an amine reactive resin, and eluted with 20 μg/ml of HA peptide, or 100 μg/ml of FLAG peptide, respectively. 30 μg of SDHB-HA were combined with 30 μg of either HSC20-FLAG or RAB5A-FLAG in buffer I2 (25 mM TrisHCl; 300 mM NaCl; 1 mM EDTA; 1% NP-40; 1% DTT; 1 mM PMSF; 5% glycerol), and incubated for 3 h at 4 ^{o}C in the presence of anti-HA beads to immunoprecipitate SDHB-HA. After extensive washing of the beads, the elution was performed with 20 μg/ml of HA peptide. The eluates after immunoprecipitations of SDHB-HA were analyzed by SDS-

PAGE and Coomassie staining. Aliquots corresponding to 33% of the inputs were run on the gel for comparison. RAB5A-FLAG was used as a negative control.

Aconitase In-gel Assay and Electrophoretic Mobility Shift Assay (EMSA)

Aconitase was assayed using a coupled assay after native PAGE separation, as previously described (Tong and Rouault, 2006).

IRP-IRE binding was determined by EMSA using a P^{32}- labeled ferritin IRE probe, as previously described (Tong and Rouault, 2006).

Immunoblots

Antibodies in these studies are as follows: anti-SDHB, SDHA, NDUFS3, MTCO1, NQO2, HELZ, UQCRFS1, SUCLG2, DNAJA2 mouse monoclonal antibodies, and anti-EPRS, SDHC, SDHD rabbit polyclonal antibodies were from Abcam. Anti-HSC20, HSPA9 rabbit polyclonal antibodies were from Sigma. Anti-LYRM7, SUCLG2 rabbit polyclonal antibodies were from Novus Biologicals. Anti-HSPA14 rabbit monoclonal, and anti-SDHAF1 rabbit polyclonal antibodies were from Origene. Mouse monoclonal anti-human TfR1 was from Zymed. Anti-IRP1, IRP2, ISCU, GLRX5, NFU1 rabbit polyclonal sera were raised against synthetic peptide fragments (Tong et al., 2003; Tong and Rouault, 2006; Ye et al., 2010). Anti-ISCU rabbit polyclonal antibody was purchased from Proteintech.

Statistical Analyses

Where applicable, data are expressed as the mean ± standard deviation. Pairwise comparisons between two groups were analyzed using the unpaired Student's *t* test.

Materials and Data

Interaction data reported in this manuscript were submitted to the DIP database and assigned IMEx Consortium Accession IM-21965.

SUPPLEMENTAL REFERENCES

Diaz, F., Barrientos, A., and Fontanesi, F. (2009). Evaluation of the mitochondrial respiratory chain and oxidative phosphorylation system using blue native gel electrophoresis. Curr Protoc Hum Genet Chapter 19, Unit19 14.

Lemarie, A., Huc, L., Pazarentzos, E., Mahul-Mellier, A.L., and Grimm, S. (2011). Specific disintegration of complex II succinate:ubiquinone oxidoreductase links pH changes to oxidative stress for apoptosis induction. Cell Death Differ 18, 338-349.

Munujos, P., Coll-Canti, J., Gonzalez-Sastre, F., and Gella, F.J. (1993). Assay of succinate dehydrogenase activity by a colorimetric-continuous method using iodonitrotetrazolium chloride as electron acceptor. Anal Biochem 212, 506-509.

Stehling, O., Sheftel, A.D., and Lill, R. (2009). Chapter 12 Controlled expression of iron-sulfur cluster assembly components for respiratory chain complexes in mammalian cells. Methods Enzymol 456, 209-231.

Tong, W.H., Jameson, G.N., Huynh, B.H., and Rouault, T.A. (2003). Subcellular compartmentalization of human Nfu, an iron-sulfur cluster scaffold protein, and its ability to assemble a [4Fe-4S] cluster. Proceedings of the National Academy of Sciences of the United States of America 100, 9762-9767.

Tong, W.H., and Rouault, T.A. (2006). Functions of mitochondrial ISCU and cytosolic ISCU in mammalian iron-sulfur cluster biogenesis and iron homeostasis. Cell Metab 3, 199-210.

Wittig, I., Carrozzo, R., Santorelli, F.M., and Schagger, H. (2007). Functional assays in high-resolution clear native gels to quantify mitochondrial complexes in human biopsies and cell lines. Electrophoresis 28, 3811-3820.

Ye, H., Jeong, S.Y., Ghosh, M.C., Kovtunovych, G., Silvestri, L., Ortillo, D., Uchida, N., Tisdale, J., Camaschella, C., and Rouault, T.A. (2010). Glutaredoxin 5 deficiency causes sideroblastic anemia by specifically impairing heme biosynthesis and depleting cytosolic iron in human erythroblasts. J Clin Invest 120, 1749-1761.